doi: 10.4149/gpb_2020044

circ_LRIG3 contributes to the progression of hepatocellular carcinoma by elevating RNF38 *via* sponging miR-449a

Xiaonan Hu[1], Kaikai Zhou[2], Sujuan Cao[1], Huan Zhu[1] and Kaihong Xie[1]

[1] *Department of Oncology, Affiliated Hospital of Xiangnan University, Chenzhou, China*
[2] *Department of General Surgery, The First People's Hospital of Chenzhou, Chenzhou, China*

Abstract. Circular RNAs (circRNAs) play crucial roles in multiple cancers, including hepatocellular carcinoma (HCC). However, the effects and molecular mechanisms of circ_LRIG3 in HCC remain barely unknown. qRT-PCR assay was employed to detect the levels of circ_LRIG3, LRIG3, miR-449a and ring finger protein 38 (RNF38). RNase R assay and Actinomycin D assay were performed to analyze the characteristics of circ_LRIG3. Colony formation assay and MTT assay were used to evaluate cell proliferation. Flow cytometry analysis and transwell assay were adopted for cell apoptosis and metastasis, respectively. Western blot assay was carried out for the protein levels of Ki67, Snail, E-cadherin, RNF38, Smad2/3 and p-Smad2/3. Murine xenograft model assay was used to explore the role of circ_LRIG3 *in vivo*. circ_LRIG3 expression was upregulated in HCC tissues and cells. Knockdown of circ_LRIG3 suppressed proliferation, migration and invasion and facilitated cell apoptosis in HCC cells *in vitro* and blocked tumor growth of HCC *in vivo*. RNF38 overexpression reversed the effects of circ_LRIG3 knockdown on the malignant behaviors of HCC cells. Moreover, circ_LRIG3 could sponge miR-449a to positively modulate RNF38 expression in HCC cells. circ_LRIG3 knockdown inhibited the progression of HCC cells by sponging miR-449a. In addition, circ_LRIG3 silencing might inhibit the Smad2/3 pathway. circ_LRIG3 facilitated HCC progression by modulation of miR-449a/LRIG3 axis, which might provide a novel method for HCC therapy.

Key words: Hepatocellular carcinoma — circ_LRIG3 — miR-449a — LRIG3 — Smad2/3

Introduction

Hepatocellular carcinoma (HCC) is a kind of primary liver cancer, ranking third leading reason of cancer-associated death in the world (Jemal et al. 2011; Siegel et al. 2017). Presently, the treatment methods, including surgery, chemotherapy, radiotherapy and biotherapy, have made great improvements, but the prognosis remains dismal due to the high incidence of metastasis and recurrence (Hao et al. 2009; Bruix et al. 2014). Thus, it is essential to explore the pathogenic mechanism of HCC and identify effective treatment methods.

Circular RNAs (circRNAs) are a family of non-coding RNAs (ncRNAs) and possess closed-loop structures (Meng et al. 2017; Zhou et al. 2018). Mounting evidence has verified that circRNAs play essential roles in malignant cancers, including HCC. For example, circ_0067934 contributed to tumor growth and metastasis in HCC by reducing miR-1324 and increasing FZD5 (Zhu et al. 2018). circ-ZEB1.33 served as a tumor promoter in HCC *via* modulation of miR-200a/CDK6 axis (Gong et al. 2018). As a member of circRNAs, circ_LRIG3 (also termed as circ_0027345) has been verified to reverse matrine-mediated effects on HCC cell behaviors (Lin et al. 2020). However, the exact roles of circ_LRIG3 in HCC remain largely undefined.

MicroRNAs (miRNAs) are a sort of ncRNAs with ~22 nucleotides and able to regulate gene expression *via* combining with the 3' untranslated region (3'UTR) of target mRNAs (He and Hannon 2004; Peng and Croce 2016). Multiple miRNAs have been demonstrated to be related to the carcinogenesis of HCC. For instance, miR-144 played a tumor-suppressive role in HCC by targeting CCNB1 (Gu et al. 2019). miR-873

Correspondence to: Kaihong Xie, Department of Oncology, Affiliated Hospital of Xiangnan University, Chenzhou, Hunan, China
E-mail: xkh001@126.com

facilitated HCC cell proliferation and metastasis by targeting TSLC1 (Han et al. 2018). Moreover, miR-449a has been verified to decelerate HCC development by interacting with ADAM10 (Liu et al. 2016), Notch1 (Han et al. 2019) and Met (Chen et al. 2015). Ring finger protein 38 (RNF38) is implicated in a variety of human diseases, including HCC (Eisenberg et al. 2002; Hu et al. 2020; Huang et al. 2020b). Nonetheless, whether RNF38 can be targeted by miR-449a is not clarified.

Herein, the expression profiles of circ_LRIG3, miR-449a and RNF38 in HCC tissues and cells were examined. Furthermore, the functions and underlying mechanisms of circ_LRIG3 in HCC were elucidated.

Materials and Methods

Tissues acquisition

The clinicopathological characteristics of HCC patients were exhibited in Table 1. 45 pairs of HCC tissues and adjacent non-tumor tissues were harvested from the patients (aged 40–70, 33 males and 12 females) with HCC at Affiliated Hospital of Xiangnan University through surgical resection and then preserved at –80°C prior to use. This work was conducted following approval was obtained from the Ethics Committee of Affiliated Hospital of Xiangnan University and written informed consents were signed by all patients.

Cell culture

The HCC cell lines (Huh7 and Hep3B) were bought from Procell (Wuhan, China) and the human normal liver cell line (THLE-2) was bought from the American Type Culture Collection (ATCC, Manassas, VA, USA). All cells were kept in Dulbecco's modified Eagle's medium (DMEM; Procell) added with 10% fetal bovine serum (FBS; Procell) and 1% penicillin-streptomycin (Procell) at 37°C in a humid incubator consisting of 5% CO_2.

Table 1. The clinicopathological characteristics of HCC patients

Parameter	Group	*n*
Age	≤50	27
	>50	18
Sex	Male	33
	Female	12
Etiology	HBV	31
	None	14
Stage	I+II	19
	III+IV	26
Tumor metastasis	Yes	30
	No	15

HCC, hepatocellular carcinoma; *n*, number of patients; HBV, hepatitis B virus

Quantitative real-time polymerase chain reaction (qRT-PCR)

Total RNA extraction was done utilizing TRIzol (Beyotime, Shanghai, China). The extracted RNAs were treated with RNase-free DNase (Promega, Madison, WI, USA) to avoid the contamination of genomic DNA. The RNA samples were quantified on a NanoDrop 2000c spectrophotometer (Thermo Fisher Scientific, Waltham, MA, USA) and then cDNAs were synthesized utilizing HiScript® II Reverse Transcriptase Kit (Vazyme, Nanjing, China) or miRNA 1st Strand cDNA Synthesis Kit (Vazyme). Next, qRT-PCR reaction was manipulated on the CFX96 Touch Real-time PCR detection system (Bio-Rad, Hercules, CA, USA) utilizing AceQ Universal SYBR qPCR Master Mix (Vazyme) and specific primers (GeneCopoeia, Guangzhou, China). The primers were: circ_LRIG3: (F: 5'-TCACTGGTTTGGATGCATTG-3' and R: 5'-AAGGTGGCTCATGGAACTTG-3'); LRIG3: (F: 5'-CAACCGAGTCACATCAATGG-3' and R: 5'-TGGGGCAGTTTAAACATCTTG-3'); miR-449a: (F: 5'-CGGCGGTTGGCAGTGTATTGTTA-3' and R: 5'-AGAGGCAGGGATGATGTTCTG-3'); RNF38: (F: 5'-GTCTGCCTCTTCCTGCAGTT-3' and R: 5'-AGGGCAAAATTGTGCTTCTG-3'); glyceraldehyde 3-phosphate dehydrogenase (GAPDH): (F: 5'-GAGTCAACGGATTTGGTCGT-3' and R: 5'-TTGATTTTGGAGGGATCTCG-3'); U6: (F: 5'-CTCGCTTCGGCAGCACA-3' and R: 5'-AACGCTTCACGAATTTGCGT-3'). The relative expression was estimated by the $2^{-\Delta\Delta Ct}$ strategy with GAPDH or U6 utilized for normalization.

RNase R and Actinomycin D experiments

For RNase R treatment, the RNA in Huh7 and Hep3B cells was treated with or without RNase R (3 U/mg; Epicentre, Madison, Wisconsin, USA) at 37°C. After 30 min, the levels of circ_LRIG3 and LRIG3 were examined by qRT-PCR assay.

To block transcription, Huh7 and Hep3B cells were exposed to Actinomycin D (2 μg/ml; Abcam, Cambridge, MA, USA) for 0, 8, 16 and 24 h. Next, the RNA in Huh7 and Hep3B cells was extracted and the enrichment of circ_LRIG3 and LRIG3 was tested.

Cell transfection

circ_LRIG3 small interfering RNA (si-circ_LRIG3) and scramble siRNA (si-NC), the overexpression vector of RNF38 (RNF38) and pcDNA empty vector (pcDNA), miR-449a mimics (miR-449a) and miR-NC, miR-449a inhibitors

(anti-miR-449a) and anti-miR-NC, circ_LRIG3 short hairpin RNA (sh-circ_LRIG3) and sh-NC were synthesized by GeneCopoeia. Cell transfection was executed through the usage of Lipofectamine 2000 (Invitrogen, Carlsbad, CA, USA).

Colony formation assay

48 h after transfection, Huh7 and Hep3B cells (200 cells/well) were placed in the 6-well plates and cultivated in culture medium for 10 days. Then the colonies were fixed in methanol and stained with 0.1% crystal violet (Solarbio, Beijing, China) for 15 min. The numbers of colonies were observed utilizing a microscope (Olympus, Tokyo, Japan) at the magnification of 40×.

3-(4, 5-dimethyl-2-thiazolyl)-2, 5-diphenyl-2-H-tetrazolium bromide (MTT) assay

After 48 h of transfection, Huh7 and Hep3B cells were harvested and then seeded into 96-well plates (1×10^4 cells/well) and cultured overnight. 20 μl MTT (5 mg/ml; Solarbio) was then added into each well of the plates at 1, 2 and 3 day with incubation for a further 4 h. Thereafter, cell supernatant was removed and 150 μl dimethyl sulfoxide (DMSO; Solarbio) was added to dissolve the formazan crystals. The absorption at 570 nm was measured with a microplate reader (Potenov, Beijing, China).

Western blot assay

The extraction of total protein was finished through the usage of RIPA buffer (Beyotime) and quantified through the usage of BCA Protein Quantification Kit (Vazyme). Then the proteins were subjected to sodium dodecyl sulfonate-polyacrylamide gel (Solarbio) electrophoresis and blotted onto polyvinylidene difluoride membranes (Amersham Biosciences, Chicago, IL, USA). Next, the membranes were blocked in 5% defatted milk for 1 h at indoor temperature and then cultivated with primary antibodies against RNF38 (ab121487; Abcam), Ki67 (ab16667; Abcam), Snail (ab53519; Abcam), E-cadherin (ab231303; Abcam), Smad2/3 (ab202445; Abcam), phospho-Smad2/3 (p-Smad2/3; ab272332; Abcam) and GAPDH (ab9485; Abcam) overnight at 4°C and secondary antibody (ab6789; Abcam) for 1.5 h at indoor temperature. The proteins were visualized with ECL reagent (Vazyme).

Flow cytometry analysis

The Annexin V-fluorescein isothiocyanate (FITC)/propidium iodide (PI) Apoptosis Detection Kit (Beyotime) was adopted to analyze HCC cell apoptosis. In short, the transfected Huh7 and Hep3B cells were seeded into 6-well plates and rinsed with cold PBS (Sangon, Shanghai, China). Next, the cells were resuspended and dyed with 5 μl Annexin V-FITC and 5 μl PI in the dark. After 15 min, the apoptotic cells were analyzed utilizing flow cytometry (Beckman Coulter, Atlanta, GA, USA).

Transwell assay

To assess cell migration ability, Huh7 and Hep3B cells (1×10^4) were suspended in serum-free medium and then plated into the upper compartment of the 24-well transwell inserts (BD Bioscience, San Jose, CA, USA). 600 μl culture medium containing 10% FBS (Procell) was supplemented into the lower compartment of the inserts. 24 h later, the migrated cells were fixed in 4% paraformaldehyde (Sangon), dyed with 0.1% crystal violet (Solarbio) and counted under an inverted microscope (Olympus) at the magnification of 100×.

To test cell invasion ability, the top compartment of the transwell inserts (BD Biosciences) was pre-coated with Matrigel (BD Biosciences) and the other procedures were consistent with those in cell migration assay.

Dual-luciferase reporter assay

The circ_LRIG3 or RNF38 3'UTR fragments consisting of the wild-type (wt) or mutant (mut) miR-449a binding sequences were cloned into pmirGLO plasmid (Promega), constructing circ_LRIG3-wt, circ_LRIG3-mut, RNF38-wt and RNF38-mut. Next, the constructs were transfected into Huh7 and Hep3B cells together with miR-449a or miR-NC. The luciferase activity was measured with a Dual-Luciferase Reporter Assay System (Promega) after 48 h.

Murine xenograft model

The 4–6 weeks old BALB/c nude mice were obtained from Vital River Laboratory (Beijing, China) and divided into 2 groups ($n = 7$). The Hep3B cells transfected with sh-NC or sh-circ_LRIG3 were subcutaneously implanted into the mice. The length (L) and width (W) of the xenograft tumor were monitored every 5 days from the 10^{th} day and tumor volume was computed with the formula: $(L\times W^2)/2$. On day 30, the mice were euthanized and the xenograft tumor weight was measured. The tumor tissues were collected and stored at −80°C. The animal study was allowed by the Ethics Committee of Animal Research of Affiliated Hospital of Xiangnan University.

Statistical analysis

The experiments were executed triple times and the results were estimated with GraphPad Prism 7. The results were

exhibited as mean ± standard deviation. Student's *t*-test or one-way analysis of variance was employed to compare the differences. The correlations among circ_LRIG3, miR-449a and RNF38 in HCC tissues were estimated by Pearson's correlation coefficient analysis. $p < 0.05$ was defined as a significant difference.

Results

circ_LRIG3 was upregulated in HCC tissues and cell lines

To clarify the roles of circ_LRIG3 in the development of HCC, the expression level of circ_LRIG3 in 50 HCC tissue specimens and adjacent normal tissue specimens was determined by qRT-PCR assay. The results showed that compared to normal tissues, circ_LRIG3 was conspicuously increased in HCC tissues (Fig. 1A). We also detected the expression level of circ_LRIG3 in HCC cells (Huh7 and Hep3B) and THLE-2 cells by qRT-PCR analysis, showing that circ_LRIG3 was highly expressed in HCC cells in comparison with THLE-2 cells (Fig. 1B). Next, RNase R assay and Actinomycin D assay were conducted to analyze the features of circ_LRIG3. RNase R assay exhibited that RNase treatment markedly decreased LRIG3 level in Huh7 and Hep3B cells, but had no effect on circ_LRIG3 level (Fig. 1C,D). Actinomycin D assay presented that circ_LRIG3 had a longer half-life than LRIG3 (Fig. 1E,F). These results indicated that circ_LRIG3 was stable and might play a role in HCC progression.

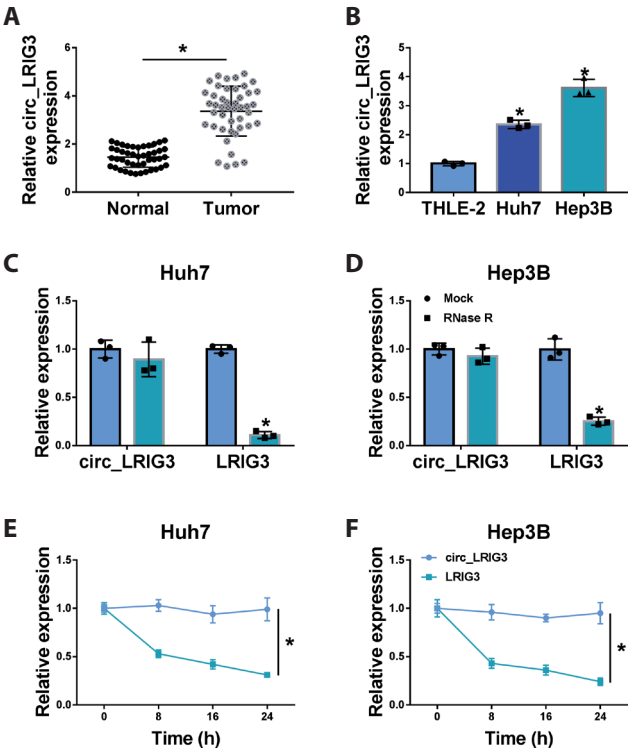

Figure 1. circ_LRIG3 was overexpressed in HCC tissues and cells. QRT-PCR assay was performed to determine the expression level of circ_LRIG3 in HCC tissues (**A**) and cells (**B**). After total RNA in Huh7 (**C**) and Hep3B (**D**) cells was treated with RNase R, the expression levels of circ_LRIG3 and LRIG3 were detected by qRT-PCR assay. Huh7and Hep3B cells were exposed to Actinomycin D at 0, 8, 16 and 24 h, and then the expression levels of circ_LRIG3 and LRIG3 in Huh7 (**E**) and Hep3B (**F**) cells were determined by qRT-PCR assay. * $p < 0.05$.

Silencing of circ_LRIG3 suppressed HCC cell proliferation, migration and invasion and promoted apoptosis

To elucidate the exact roles of circ_LRIG3 in HCC development, loss-of-function experiments were conducted through transfecting si-circ_LRIG3 into Huh7 and Hep3B cells. As shown in Figure 2A and B, si-circ_LRIG3 transfection led to an obvious reduction in circ_LRIG3 level in both Huh7 and Hep3B cells compared to si-NC groups. Colony formation assay showed that the colony formation ability of Huh7 and Hep3B cells was evidently restrained by decreasing circ_LRIG3 compared to control groups (Fig. 2C). MTT assay indicated that the proliferation of Huh7 and Hep3B cells was markedly repressed by the reduction of circ_LRIG3 in comparison with si-NC control groups (Fig. 2D,E). Then Western blot assay was conducted to measure the level of proliferation-related protein Ki67, exhibiting that circ_LRIG3 knockdown decreased Ki67 protein level in both Huh7 and Hep3B cells (Fig. 2F). As demonstrated by flow cytometry analysis, circ_LRIG3 deficiency facilitated the apoptosis of Huh7 and Hep3B cells compared to control groups (Fig. 2G). The results of transwell assay showed that cell migration and invasion in Huh7 and Hep3B cells were apparently repressed by the downregulation of circ_LRIG3 (Fig. 2H,I). Furthermore, we determined the levels of metastasis-associated proteins (Snail and E-cadherin) in Huh7 and Hep3B cells *via* Western blot assay. The results exhibited that circ_LRIG3 knockdown prominently reduced Snail level and enhanced E-cadherin level in Huh7 and Hep3B cells compared to control groups (Fig. 2J,K). Collectively, circ_LRIG3 knockdown played an anti-tumor role in HCC progression.

Overexpression of RNF38 rescued the effects of circ_LRIG3 knockdown on the malignant behaviors of HCC cells

As we observed in Figure 3A and B, circ_LRIG3 knockdown drastically decreased the mRNA and protein levels of RNF38 in Huh7 and Hep3B cells, whereas the transfection of RNF38 reversed the effects. The results of colony formation assay and MTT assay indicated that circ_LRIG3

knockdown notably inhibited cell colony formation and proliferation in Huh7 and Hep3B cells, while the effects were partially overturned by elevating RNF38 level (Fig. 3C–E). Moreover, we found that the reduction of Ki67 level in Huh7 and Hep3B cells caused by circ_LRIG3 knockdown was ameliorated by the overexpression of

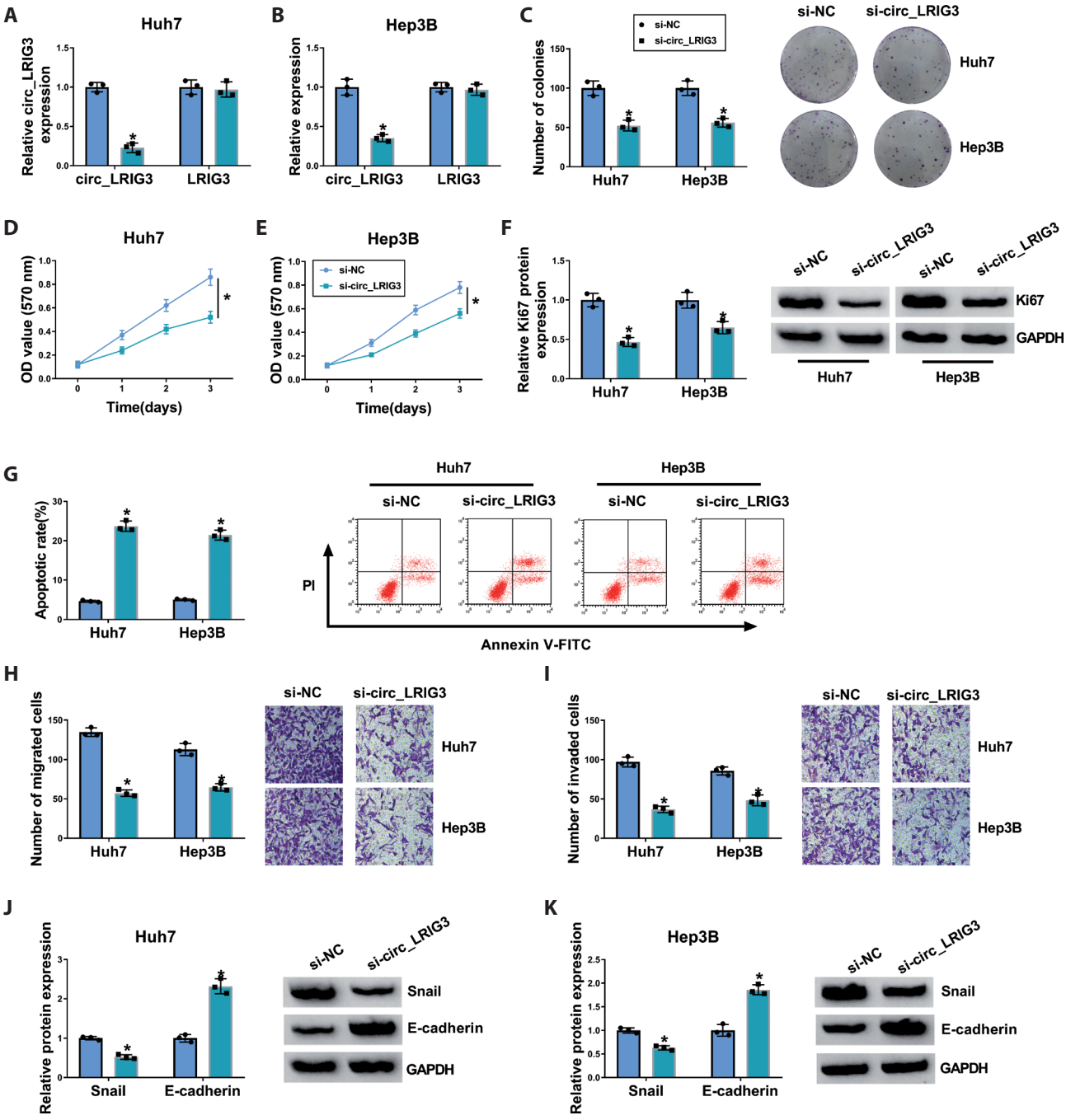

Figure 2. Effects of circ_LRIG3 on the malignant behaviors of HCC cells. Huh7 and Hep3B cells were transfected with si-circ_LRIG3 or si-NC. The expression levels of circ_LRIG3 and LRIG3 in Huh7 (**A**) and Hep3B (**B**) cells were detected *via* qRT-PCR assay. **C–E.** The colony formation and proliferation capacities of Huh7 and Hep3B cells were evaluated by colony formation assay and MTT assay, respectively. **F.** The protein level of Ki67 in Huh7 and Hep3B cells was measured *via* Western blot assay. **G.** The apoptosis of Huh7 and Hep3B cells was analyzed by flow cytometry analysis. The migration (**H**) and invasion (**I**) of Huh7 and Hep3B cells were assessed by transwell assay. The protein levels of Snail and E-cadherin in Huh7 (**J**) and Hep3B (**K**) cells were measured by Western blot assay. * $p < 0.05$. OD, optical density.

RNF38 (Fig. 3F). Flow cytometry analysis and transwell assay indicated that the promotional effect of circ_LRIG3 knockdown on cell apoptosis and the suppressive effects of circ_LRIG3 knockdown on cell migration and invasion in Huh7 and Hep3B cells were all abrogated by increasing RNF38 (Fig. 3G–I). Additionally, Western blot assay showed that the impacts of circ_LRIG3 silencing on the protein levels of Snail and E-cadherin in Huh7 and Hep3B cells were also attenuated by the elevation of RNF38 (Fig. 3J,K). Taken together, RNF38 overexpression weakened circ_LRIG3 knockdown-mediated inhibitory effect on HCC cell progression.

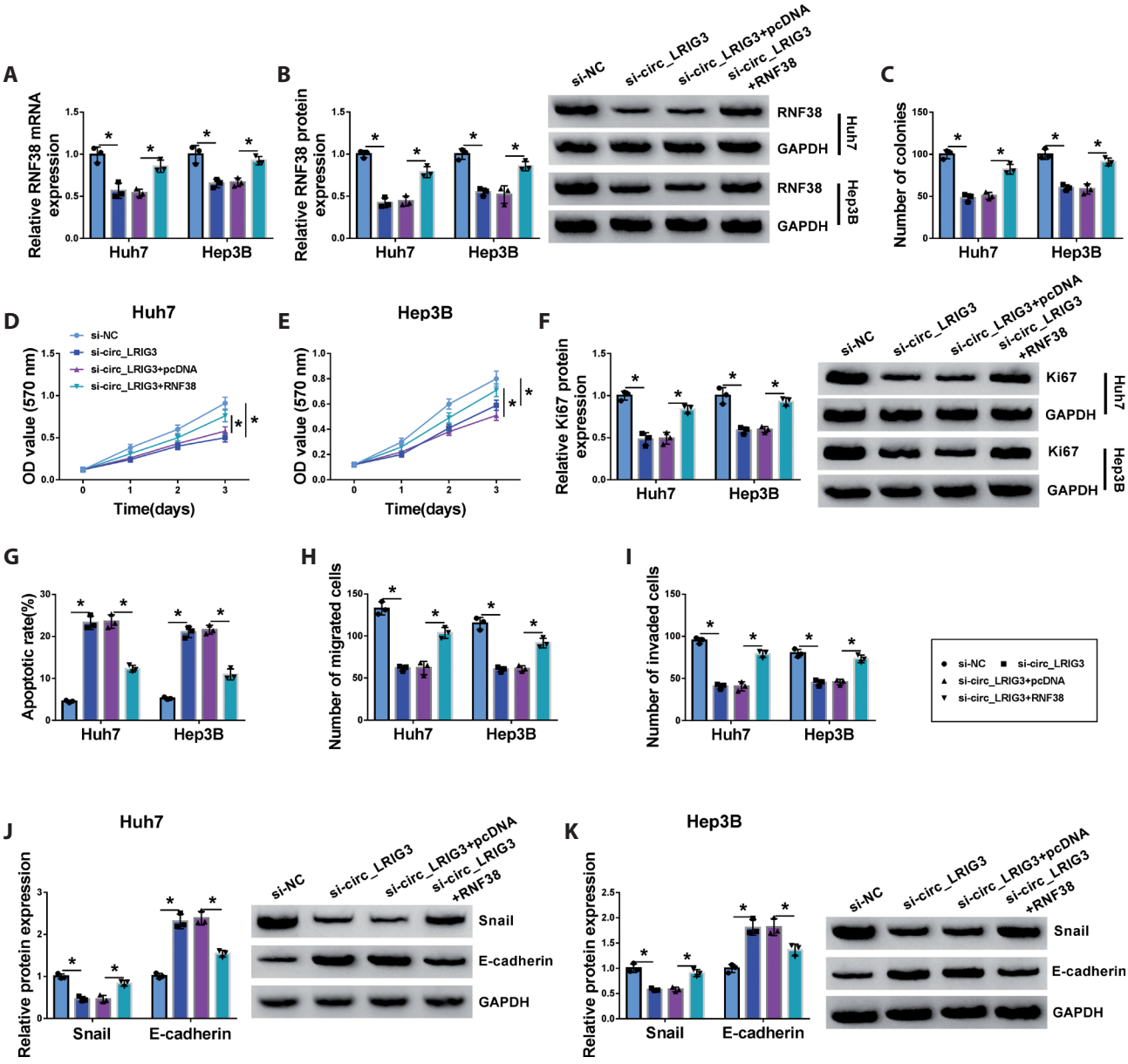

Figure 3. RNF38 overexpression reversed the suppressive role of circ_LRIG3 silencing in HCC cell progression. Huh7 and Hep3B cells were transfected with si-NC, si-circ_LRIG3, si-circ_LRIG3+pcDNA or si-circ_LRIG3+RNF38. The mRNA (**A**) and protein (**B**) levels of RNF38 in Huh7 and Hep3B cells were measured by qRT-PCR assay and Western blot assay, respectively. **C–E.** The colony formation and proliferation capacities of Huh7 and Hep3B cells were assessed by colony formation assay and MTT assay, respectively. **F.** The protein level of Ki67 in Huh7 and Hep3B cells was examined by Western blot assay. **G.** The apoptosis of Huh7 and Hep3B cells was assessed by flow cytometry analysis. The migration (**H**) and invasion (**I**) abilities of Huh7 and Hep3B cells were measured by transwell assay. The protein levels of Snail and E-cadherin in Huh7 (**J**) and Hep3B (**K**) cells were determined by Western blot assay. * $p < 0.05$.

circ_LRIG3 positively regulated RNF38 expression by sponging miR-449a

In order to explore the association between circ_LRIG3 and RNF38 in the regulation of HCC progression, we firstly searched online software circbank and found that miR-449a contained the binding sites of circ_LRIG3, indicating that miR-449a might be a target of circ_LRIG3 (Fig. 4A). Then we performed dual-luciferase reporter assay to verify the interaction between circ_LRIG3 and miR-449a. The results showed that miR-449a transfection drastically inhibited the luciferase activity of circ_LRIG3-wt in both Huh7 and Hep3B cells, but there was no change in the luciferase activity of circ_LRIG3-mut (Fig. 4B,C). Moreover, we observed that circ_LRIG3 knockdown markedly elevated the expression level of miR-449a in Huh7 and Hep3B cells (Fig. 4D). In addition, a low expression of miR-449a was observed in HCC cells and tissues compared to normal cells and tissues (Fig. 4E,F). As estimated by Pearson's correlation coefficient analysis, there was an inverse correlation between the levels of miR-449a and circ_LRIG3 in HCC tissues (Fig. 4G).

Interestingly, through analyzing online tool miRDB, RNF38 was found to be a target gene of miR-449a and their potential binding sites were exhibited in Figure 4H. The results of dual-luciferase reporter assay showed that the luciferase activity in miR-449a and RNF38-wt co-transfected Huh7 and Hep3B cells was apparently suppressed compared to miR-NC and RNF38-wt co-transfected groups, but the luciferase activity was not changed in RNF38-mut groups, further demonstrating the interaction between RNF38 and miR-449a (Fig. 4I,J). Next, miR-NC, miR-449a, anti-miR-NC or anti-miR-449a was transfected into Huh7 and Hep3B cells to analyze the relationship between miR-449a and RNF38 in HCC cells. As shown in Figure 4K and M, miR-449a transfection led to a remarkable increase in miR-449a expression level and a noteworthy decrease in RNF38 mRNA and protein levels in Huh7 and Hep3B cells, while the transfection of anti-miR-449a exhibited the opposite results. Moreover, our results exhibited that the mRNA and protein levels of RNF38 were all enhanced in Huh7 and Hep3B cells compared to THLE-2 cells (Fig. 4N,O). The mRNA and protein levels of RNF38 were also increased in HCC tissues compared to normal tissues (Fig. 4P,S). Additionally, we found that RNF38 mRNA level was negatively correlated with miR-449a level and positively correlated with circ_LRIG3 level in HCC tissues (Fig. 4Q,R).

Thereafter, our results presented that circ_LRIG3 silencing evidently reduced the mRNA and protein levels of RNF38 in Huh7 and Hep3B cells, while the transfection of anti-miR-449a abrogated the impacts (Fig. 4T,U). All these results suggested that circ_LRIG3 could facilitate RNF38 expression by targeting miR-449a.

circ_LRIG3 knockdown repressed HCC cell progression by targeting miR-449a

To further investigate the functional roles of circ_LRIG3 and miR-449a in HCC development, Huh7 and Hep3B cells were assigned to 4 groups: si-NC, si-circ_LRIG3, si-circ_LRIG3+anti-miR-NC and si-circ_LRIG3+anti-miR-449a. As presented in Figure 5A, si-circ_LRIG3 transfection resulted in an obvious elevation in miR-449a level in Huh7 and Hep3B cells, while anti-miR-449a transfection reversed this effect. The results of colony formation assay and MTT assay indicated that miR-449a inhibition abated the suppressive roles of circ_LRIG3 knockdown in the colony formation and proliferation abilities of Huh7 and Hep3B cells (Fig. 5B–D). The reduced protein level of Ki67 in Huh7 and Hep3B cells mediated by circ_LRIG3 deficiency was also reversed by decreasing miR-449a (Fig. 5E). As illustrated by flow cytometry analysis and transwell assay, circ_LRIG3 silencing promoted cell apoptosis and inhibited cell migration and invasion in Huh7 and Hep3B cells, whereas miR-449a inhibition partially overturned the effects (Fig. 5F–H). Furthermore, miR-449a inhibition reversed the inhibitory effect on Snail level and the promotional effect on E-cadherin in Huh7 and Hep3B cells mediated by circ_LRIG3 deficiency (Fig. 5I,J). To summarize, circ_LRIG3 knockdown repressed the malignant behaviors of HCC cells by targeting miR-449a.

circ_LRIG3 knockdown might inhibit the Smad2/3 pathway

We then determined the phosphorylation level of Smad2/3 in Huh7 and Hep3B cells transfected with si-NC, si-circ_LRIG3, si-circ_LRIG3+anti-miR-NC, si-circ_LRIG3+anti-miR-449a, si-circ_LRIG3+pcDNA or si-circ_LRIG3+RNF38 using Western blot assay. The results showed that circ_LRIG3 knockdown reduced the level of p-Smad2/3 in both Huh7 and Hep3B cells, indicating the Smad2/3 pathway might be blocked; however, miR-449a inhibition or RNF38 overexpression partially abrogated the effect (Fig. 6A,B). Thus, it was concluded that circ_LRIG3 might promote the Smad2/3 pathway through regulating miR-449a and RNF38.

circ_LRIG3 knockdown hampered tumorigenesis of HCC in vivo

To clarify the roles of circ_LRIG3 in tumor growth *in vivo*, the murine xenograft model was established by injecting sh-circ_LRIG3 or sh-NC transfected Hep3B cells into the mice. The mice with sh-circ_LRIG3 transfected Hep3B cells showed a decreased tumor volume and weight in comparison with sh-NC control groups (Fig. 7A,B). Moreover, we found that the levels of circ_LRIG3, RNF38 mRNA and RNF38

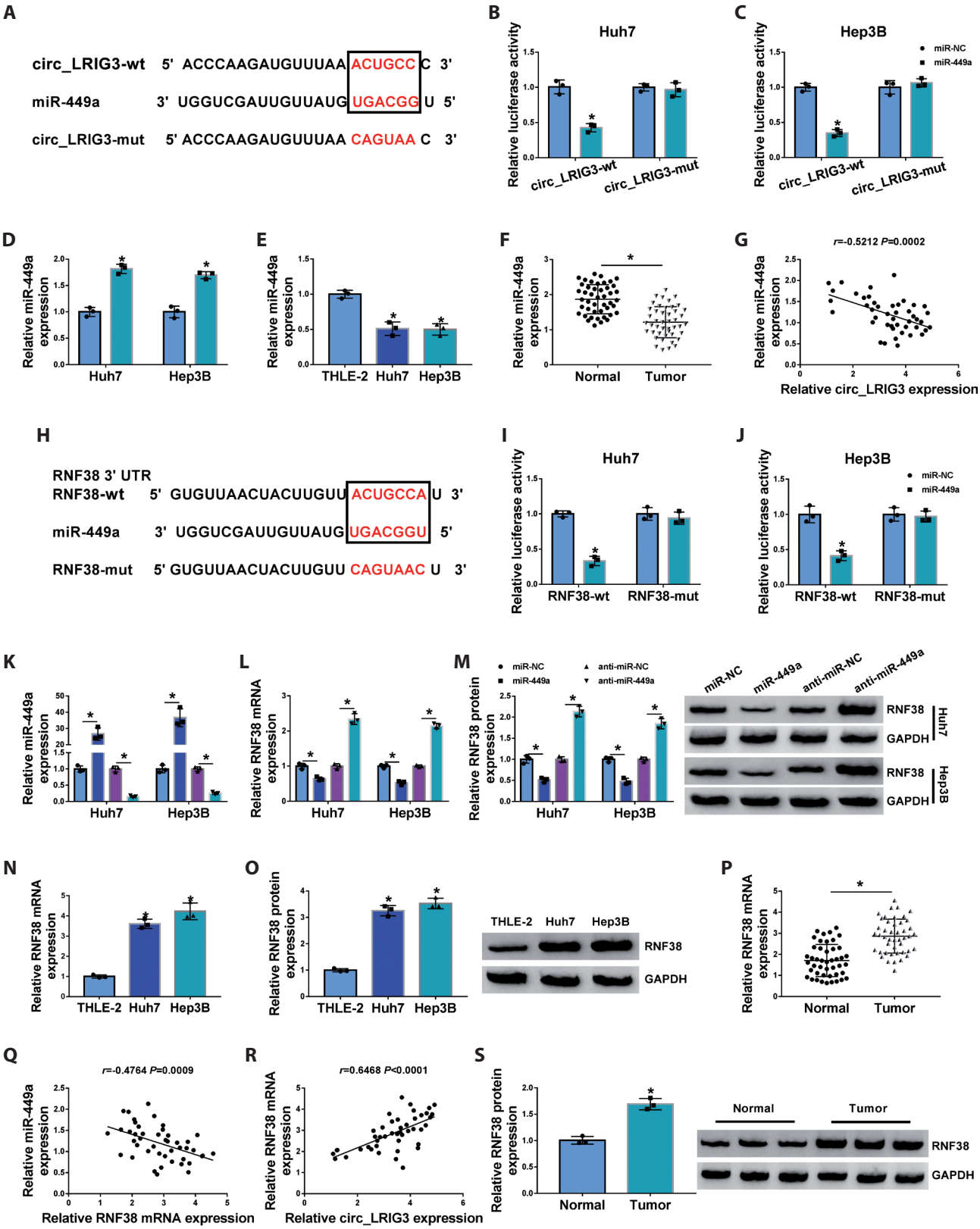
A
circ_LRIG3-wt 5' ACCCAAGAUGUUUAA ACUGCC C 3'
miR-449a 3' UGGUCGAUUGUUAUG UGACGG U 5'
circ_LRIG3-mut 5' ACCCAAGAUGUUUAA CAGUAA C 3'
B
Huh7
Relative luciferase activity
circ_LRIG3-wt
circ_LRIG3-mut
C
Hep3B
miR-NC
miR-449a
Relative luciferase activity
circ_LRIG3-wt
circ_LRIG3-mut
D
Relative miR-449a expression
Huh7
Hep3B
E
Relative miR-449a expression
THLE-2 Huh7 Hep3B
F
Relative miR-449a expression
Normal Tumor
G
r=-0.5212 P=0.0002
Relative miR-449a expression
Relative circ_LRIG3 expression
H
RNF38 3' UTR
RNF38-wt 5' GUGUUAACUACUUGUU ACUGCCA U 3'
miR-449a 3' UGGUCGAUUGUUAUG UGACGGU 5'
RNF38-mut 5' GUGUUAACUACUUGUU CAGUAAC U 3'
I
Huh7
Relative luciferase activity
RNF38-wt
RNF38-mut
J
Hep3B
miR-NC
miR-449a
Relative luciferase activity
RNF38-wt
RNF38-mut
K
Relative miR-449a expression
Huh7
Hep3B
L
Relative RNF38 mRNA expression
Huh7
Hep3B
M
miR-NC
miR-449a
anti-miR-NC
anti-miR-449a
Relative RNF38 protein expression
Huh7
Hep3B
miR-NC
miR-449a
anti-miR-NC
anti-miR-449a
RNF38
GAPDH
Huh7
RNF38
GAPDH
Hep3B
N
Relative RNF38 mRNA expression
THLE-2 Huh7 Hep3B
O
Relative RNF38 protein expression
THLE-2 Huh7 Hep3B
THLE-2 Huh7 Hep3B
RNF38
GAPDH
P
Relative RNF38 mRNA expression
Normal Tumor
Q
r=-0.4764 P=0.0009
Relative miR-449a expression
Relative RNF38 mRNA expression
R
r=0.6468 P<0.0001
Relative RNF38 mRNA expression
Relative circ_LRIG3 expression
S
Relative RNF38 protein expression
Normal Tumor
Normal
Tumor
RNF38
GAPDH

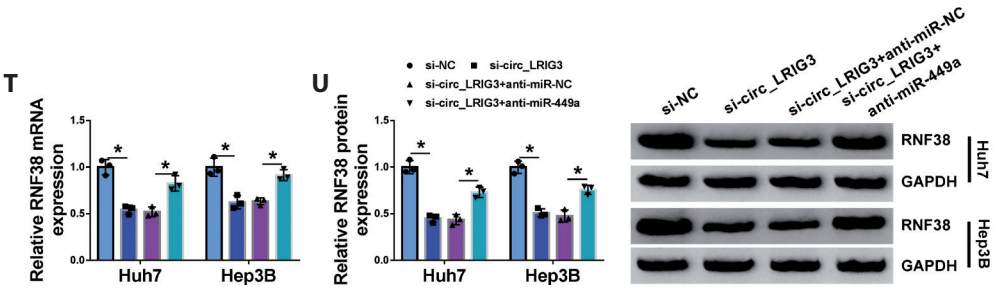

Figure 4. circ_LRIG3 directly targeted miR-449a to positively regulate RNF38 expression in HCC cells. **A.** The potential binding sites between circ_LRIG3 and miR-449a were exhibited in Huh7 (**B**) and Hep3B (**C**) cells. The interaction between circ_LRIG3 and miR-449a was verified by dual-luciferase reporter assay. **D.** The expression level of miR-449a in Huh7 and Hep3B cells transfected with si-NC or si-circ_LRIG3 was determined *via* qRT-PCR assay. The expression level of miR-449a in HCC cells (**E**) and tissues (**F**) was examined using qRT-PCR assay. **G.** The correlation between miR-449a and circ_LRIG3 in HCC tissues was estimated by Pearson's correlation coefficient analysis. **H.** The binding sequences between RNF38 and miR-449a were presented. **I, J.** The combination between RNF38 and miR-449a was demonstrated by dual-luciferase reporter assay. After Huh7 and Hep3B cells were transfected with miR-NC, miR-449a, anti-miR-NC or anti-miR-449a, the levels of miR-449a (**K**), RNF38 mRNA (**L**) and RNF38 (**M**) protein were measured by qRT-PCR assay or Western blot assay. The mRNA (**N**) and protein (**O**) levels of RNF38 in THLE-2, Huh7 and Hep3B cells were measured by qRT-PCR assay and Western blot assay, respectively. **P.** The mRNA level of RNF38 in HCC tissues and normal tissues was determined by qRT-PCR assay. The correlation between RNF38 mRNA and miR-449a (**Q**) or circ_LRIG3 (**R**) in HCC tissues was analyzed by Pearson's correlation coefficient analysis. **S.** The protein level of RNF38 in tumor tissues and normal tissues was measured *via* Western blot assay. Si-NC, si-circ_LRIG3, si-circ_LRIG3+anti-miR-NC or si-circ_LRIG3+anti-miR-449a was transfected into Huh7 and Hep3B cells, and then the mRNA (**T**) and protein (**U**) levels of RNF38 were detected through qRT-PCR assay or Western blot assay. * $p < 0.05$.

protein levels were all downregulated and the level of miR-449a was increased in the tumor tissues of sh-circ_LRIG3 groups compared to control groups (Fig. 7C–F). All these outcomes suggested that circ_LRIG3 contributed to tumor progression *in vivo*.

Discussion

Previous studies have shown that circRNAs are linked to the development of human tumors. In this paper, we devoted to exploring the roles of circ_LRIG3 in the carcinogenesis of HCC. As a result, downregulation of circ_LRIG3 restrained malignant HCC cell phenotypes. Moreover, we found that circ_LRIG3 could alter HCC progression through miR-449a/RNF38 axis and Smad2/3 pathway.

Currently, more and more reports have shown that circRNAs are abnormally expressed in HCC and regulate the malignant phenotypes of HCC cells through the competitive endogenous RNAs (ceRNAs) mechanism of circRNA/miRNA/mRNA axis (Rong et al. 2017). For example, circ_0009910 level was raised in HCC and facilitated the growth and motility of HCC cells through miR-335-5p/ROCK1 axis (Li and Liu 2020). circ_101280 level was raised in HCC and accelerated the tumorigenicity of HCC through modulation of miR-375/JAK2 axis (Cao et al. 2019). As for circ_LRIG3 (circ_0027345), Lin et al. (2020) reported that circ_0027345 inhibited autophagy and promoted growth and metastasis in matrine-treated HCC cells by modulating miR-345-3p and HOXD3. Herein, we observed that there was an upregulation of circ_LRIG3 in HCC tissue samples and cell lines. Functionally, silencing of circ_LRIG3 led to a distinct suppression in HCC cell proliferation and a marked induction in apoptosis. circ_LRIG3 silencing also repressed HCC cell migration and invasion, concomitant with downregulation of Snail and upregulation of E-cadherin. Moreover, our results showed circ_LRIG3 deficiency hampered the tumorigenicity of HCC *in vivo*. All these observations indicated that circ_LRIG3 functioned as a tumor promotor in HCC.

High level of RNF38 has been verified to accelerate the carcinogenesis of HCC (Peng et al. 2019; Hu et al. 2020). In this research, RNF38 elevation effectively ameliorated the influence of circ_LRIG3 knockdown on HCC cell proliferation, apoptosis and metastasis. Therefore, we further explored the association between circ_LRIG3 and RNF38. Our results presented that circ_LRIG3 could positively regulate RNF38 expression *via* acting as the sponge for miR-449a. Moreover, our study exhibited that miR-449a suppression rescued the influence of circ_LRIG3 deficiency on HCC cell progression, suggesting that circ_LRIG3 could accelerate the malignancy of HCC by sponging miR-449a. Han et al. (2019) disclosed that miR-449a repressed the invasiveness of HCC cells by binding to Notch1. Liu et al. (2016) manifested that miR-449a level was declined and its elevation blocked the

growth and motility of HCC cells by binding to ADAM10. Here, we identified that miR-449a could target RNF38 for the first time.

TGF-β plays a vital role in tumor progression and Smad2 and Smad3 are receptor-associated R-Smads which can form the classical TGF-β signaling cascade (Schon and

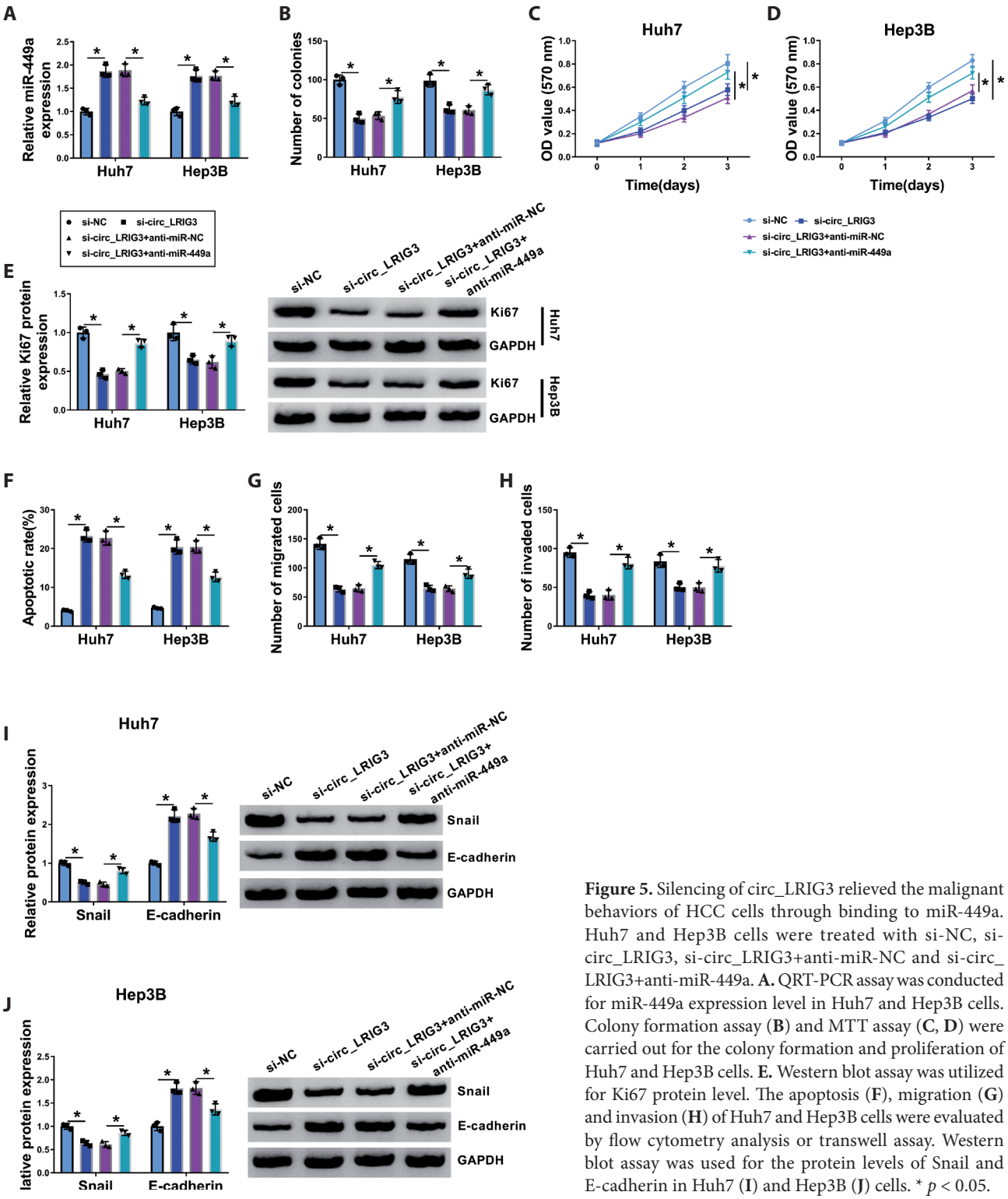

Figure 5. Silencing of circ_LRIG3 relieved the malignant behaviors of HCC cells through binding to miR-449a. Huh7 and Hep3B cells were treated with si-NC, si-circ_LRIG3, si-circ_LRIG3+anti-miR-NC and si-circ_LRIG3+anti-miR-449a. **A.** QRT-PCR assay was conducted for miR-449a expression level in Huh7 and Hep3B cells. Colony formation assay (**B**) and MTT assay (**C**, **D**) were carried out for the colony formation and proliferation of Huh7 and Hep3B cells. **E.** Western blot assay was utilized for Ki67 protein level. The apoptosis (**F**), migration (**G**) and invasion (**H**) of Huh7 and Hep3B cells were evaluated by flow cytometry analysis or transwell assay. Western blot assay was used for the protein levels of Snail and E-cadherin in Huh7 (**I**) and Hep3B (**J**) cells. * $p < 0.05$.

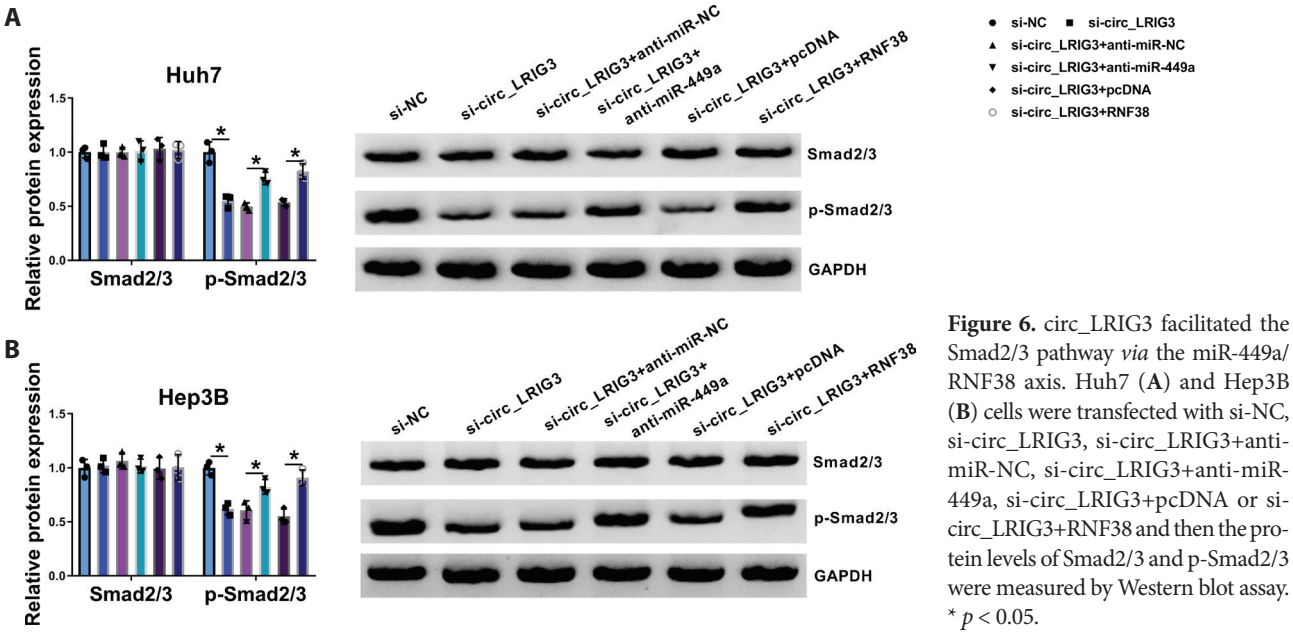

Figure 6. circ_LRIG3 facilitated the Smad2/3 pathway *via* the miR-449a/RNF38 axis. Huh7 (**A**) and Hep3B (**B**) cells were transfected with si-NC, si-circ_LRIG3, si-circ_LRIG3+anti-miR-NC, si-circ_LRIG3+anti-miR-449a, si-circ_LRIG3+pcDNA or si-circ_LRIG3+RNF38 and then the protein levels of Smad2/3 and p-Smad2/3 were measured by Western blot assay. * $p < 0.05$.

Weiskirchen 2014; Morikawa et al. 2016). TGF-β-stimulated activation of Smad2/3 is a classical pathway that induces epithelial-mesenchymal transition (EMT) (Xu et al. 2009). Moreover, the activation of TGF-β/Smad2/3 is involved in HCC progression (Yang et al. 2018; Huang et al. 2020a). Interestingly, our results showed that circ_LRIG3 knockdown decreased the phosphorylation of Smad2/3, while miR-449a suppression or RNF38 elevation reversed the effect. The results indicated that circ_LRIG3 knockdown might inactivate the Smad2/3 pathway; however, the underlying mechanism still needs to be further explored.

In summary, circ_LRIG3 level was elevated in HCC. Moreover, it was reasonable to conclude that silencing of circ_LRIG3 retarded HCC progression by regulating miR-449a/RNF38/Smad2/3 axis, which might offer a potential therapeutic strategy for HCC.

Conflict of interest. The authors declare that they have no financial conflicts of interest.

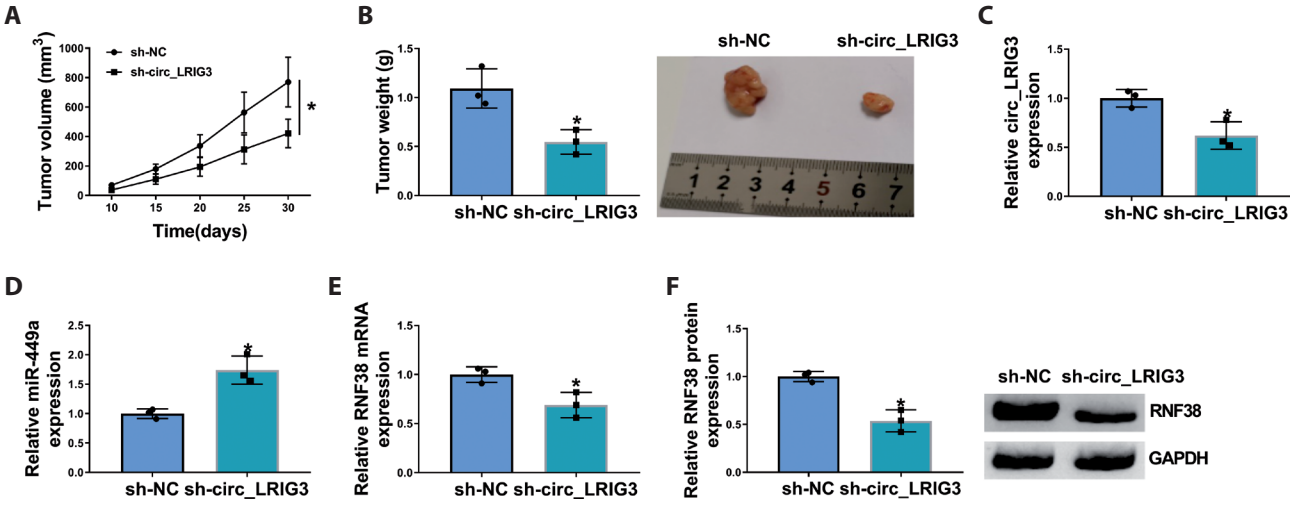

Figure 7. circ_LRIG3 silencing repressed tumorigenesis of HCC *in vivo*. **A.** Tumor volume was examined every 5 days from the 10th day after injection of sh-circ_LRIG3 or sh-NC transfected Hep3B cells. **B.** Tumor weight was examined on day 30. The levels of circ_LRIG3 (**C**), miR-449a (**D**) and RNF38 mRNA (**E**) in the collected tissues were determined by qRT-PCR assay. **F.** The protein level of RNF38 in the collected tissues was measured by Western blot assay. * $p < 0.05$.

References

Bruix J, Gores GJ, Mazzaferro V (2014): Hepatocellular carcinoma: clinical frontiers and perspectives. Gut **63,** 844-855 https://doi.org/10.1136/gutjnl-2013-306627

Cao S, Wang G, Wang J, Li C, Zhang L (2019): Hsa_circ_101280 promotes hepatocellular carcinoma by regulating miR-375/JAK2. Immunol. Cell Biol. **97,** 218-228 https://doi.org/10.1111/imcb.12213

Chen SP, Liu BX, Xu J, Pei XF, Liao YJ, Yuan F, Zheng F (2015): MiR-449a suppresses the epithelial-mesenchymal transition and metastasis of hepatocellular carcinoma by multiple targets. BMC Cancer **15,** 706 https://doi.org/10.1186/s12885-015-1738-3

Eisenberg I, Hochner H, Levi T, Yelin R, Kahan T, Mitrani-Rosenbaum S (2002): Cloning and characterization of a novel human gene RNF38 encoding a conserved putative protein with a RING finger domain. Biochem. Biophys. Res. Commun. **294,** 1169-1176 https://doi.org/10.1016/S0006-291X(02)00584-3

Gong Y, Mao J, Wu D, Wang X, Li L, Zhu L, Song R (2018): Circ-ZEB1.33 promotes the proliferation of human HCC by sponging miR-200a-3p and upregulating CDK6. Cancer Cell Int. **18,** 116 https://doi.org/10.1186/s12935-018-0602-3

Gu J, Liu X, Li J, He Y (2019): MicroRNA-144 inhibits cell proliferation, migration and invasion in human hepatocellular carcinoma by targeting CCNB1. Cancer Cell Int. **19,** 15 https://doi.org/10.1186/s12935-019-0729-x

Han B, Huang J, Yang Z, Zhang J, Wang X, Xu N, Meng H, Wu J, Huang Q, Yang X et al (2019): miR-449a is related to short-term recurrence of hepatocellular carcinoma and inhibits migration and invasion by targeting Notch1. Onco. Targets Ther. **12,** 10975-10987 https://doi.org/10.2147/OTT.S216997

Han G, Zhang L, Ni X, Chen Z, Pan X, Zhu Q, Li S, Wu J, Huang X, Wang X (2018): MicroRNA-873 promotes cell proliferation, migration, and invasion by directly targeting TSLC1 in hepatocellular carcinoma. Cell. Physiol. Biochem. **46,** 2261-2270 https://doi.org/10.1159/000489594

Hao K, Luk JM, Lee NP, Mao M, Zhang C, Ferguson MD, Lamb J, Dai H, Ng IO, Sham PC et al. (2009): Predicting prognosis in hepatocellular carcinoma after curative surgery with common clinicopathologic parameters. BMC Cancer **9,** 389 https://doi.org/10.1186/1471-2407-9-389

He L, Hannon GJ (2004): MicroRNAs: small RNAs with a big role in gene regulation. Nat. Rev. Genet. **5,** 522-531 https://doi.org/10.1038/nrg1379

Hu PA, Miao YY, Yu S, Guo N (2020): Long non-coding RNA SNHG5 promotes human hepatocellular carcinoma progression by regulating miR-363-3p/RNF38 axis. Eur. Rev. Med. Pharmacol. Sci. **24,** 3592-3604

Huang WJ, Tian XP, Bi SX, Zhang SR, He TS, Song LY, Yun JP, Zhou ZG, Yu RM, Li M (2020a): The beta-catenin/TCF-4-LINC01278-miR-1258-Smad2/3 axis promotes hepatocellular carcinoma metastasis. Oncogene **39,** 4538-4550 https://doi.org/10.1038/s41388-020-1307-3

Huang Z, Yang P, Ge H, Yang C, Cai Y, Chen Z, Tian W, Wang H (2020b): RING finger protein 38 mediates LIM domain binding 1 degradation and regulates cell growth in colorectal cancer. Onco. Targets Ther. **13,** 371-379 https://doi.org/10.2147/OTT.S234828

Li HW, Liu J (2020): Circ_0009910 promotes proliferation and metastasis of hepatocellular carcinoma cells through miR-335-5p/ROCK1 axis. Eur. Rev. Med. Pharmacol. Sci. **24,** 1725-1735

Lin S, Zhuang J, Zhu L, Jiang Z (2020): Matrine inhibits cell growth, migration, invasion and promotes autophagy in hepatocellular carcinoma by regulation of circ_0027345/miR-345-5p/HOXD3 axis. Cancer Cell Int. **20,** 246 https://doi.org/10.1186/s12935-020-01293-w

Liu S, Liu K, Zhang W, Wang Y, Jin Z, Jia B, Liu Y (2016): miR-449a inhibits proliferation and invasion by regulating ADAM10 in hepatocellular carcinoma. Am. J. Transl. Res. **8,** 2609-2619

Meng S, Zhou H, Feng Z, Xu Z, Tang Y, Li P, Wu M (2017): CircRNA: functions and properties of a novel potential biomarker for cancer. Mol. Cancer **16,** 94 https://doi.org/10.1186/s12943-017-0663-2

Morikawa M, Derynck R, Miyazono K (2016): TGF-beta and the TGF-beta Family: Context-Dependent Roles in Cell and Tissue Physiology. Cold Spring Harb. Perspect. Biol. **8,** a021873 https://doi.org/10.1101/cshperspect.a021873

Peng R, Zhang PF, Yang X, Wei CY, Huang XY, Cai JB, Lu JC, Gao C, Sun HX, Gao Q et al (2019): Overexpression of RNF38 facilitates TGF-beta signaling by ubiquitinating and degrading AHNAK in hepatocellular carcinoma. J. Exp. Clin. Cancer Res. **38,** 113 https://doi.org/10.1186/s13046-019-1113-3

Peng Y, Croce CM (2016): The role of MicroRNAs in human cancer. Signal Transduct. Target Ther. **1,** 15004 https://doi.org/10.1038/sigtrans.2015.4

Rong D, Sun H, Li Z, Liu S, Dong C, Fu K, Tang W, Cao H (2017): An emerging function of circRNA-miRNAs-mRNA axis in human diseases. Oncotarget **8,** 73271-73281 https://doi.org/10.18632/oncotarget.19154

Schon HT, Weiskirchen R (2014): Immunomodulatory effects of transforming growth factor-beta in the liver. Hepatobiliary Surg. Nutr. **3,** 386-406

Xu J, Lamouille S, Derynck R (2009): TGF-beta-induced epithelial to mesenchymal transition. Cell Res. **19,** 156-172 https://doi.org/10.1038/cr.2009.5

Yang Y, Liu Q, Li Z, Zhang R, Jia C, Yang Z, Zhao H, Ya S, Mao R, Ailijiang T, et al. (2018): GP73 promotes epithelial-mesenchymal transition and invasion partly by activating TGF-beta1/Smad2 signaling in hepatocellular carcinoma. Carcinogenesis **39,** 900-910 https://doi.org/10.1093/carcin/bgy010

Zhou R, Wu Y, Wang W, Su W, Liu Y, Wang Y, Fan C, Li X, Li G, Li Y, et al. (2018): Circular RNAs (circRNAs) in cancer. Cancer Lett. **425,** 134-142 https://doi.org/10.1016/j.canlet.2018.03.035

Zhu Q, Lu G, Luo Z, Gui F, Wu J, Zhang D, Ni Y (2018): CircRNA circ_0067934 promotes tumor growth and metastasis in hepatocellular carcinoma through regulation of miR-1324/FZD5/Wnt/beta-catenin axis. Biochem. Biophys. Res. Commun. **497,** 626-632 https://doi.org/10.1016/j.bbrc.2018.02.119

Received: June 13, 2020
Final version accepted: December 16, 2020